Two hardening mechanisms in single crystal thin films studied by discrete dislocation plasticity

Nicola, L; Van der Giessen, E; Needleman, A

Published in:
Philosophical Magazine

DOI:
10.1080/14786430500036611

Philosophical Magazine,
Vol. 85, No. 14, 11th May 2005, 1507–1518

Taylor & Francis
Taylor & Francis Group

Two hardening mechanisms in single crystal thin films studied by discrete dislocation plasticity

L. NICOLA†, E. VAN DER GIESSEN*† and A. NEEDLEMAN‡

†The Netherlands Institute for Metals Research/Department of Applied Physics, University of Groningen, Nyenborgh 4, 9747 AG Groningen, The Netherlands
‡Division of Engineering, Brown University, Providence, RI 02912, USA

(*Received 10 June 2004; in final form 23 November 2004*)

Two-dimensional discrete dislocation plasticity simulations of the evolution of thermal stress in single crystal thin films on a rigid substrate are used to study size effects. The relation between the residual stress and the dislocation structure in the films after cooling is analyzed using dislocation dynamics. A boundary layer characterized by a high stress gradient and a high dislocation density is found close to the impenetrable film-substrate interface. There is a material-dependent threshold film thickness above which the dislocation density together with the boundary layer thickness and stress state are independent of film thickness. In such films the stress outside the boundary layer is on average very low, so that the film-thickness-independent boundary layer is responsible for the size effect. A larger size effect is found for films thinner than the threshold thickness. The origin of this size effect stems from nucleation activity being hindered by the geometrical constraint of the small film thickness, so that by decreasing film thickness, the dislocation density decreases while the stress in the film increases. The size dependence is only described by a Hall–Petch type relation for films thicker than the threshold value.

1. Introduction

Even though it is widely accepted that thin film hardening is thickness dependent (e.g. Arzt [1]), a universal scaling law to describe the phenomenon has not yet been found. Many authors propose to use a Hall–Petch type relation, with the grain size replaced by the film thickness h. The exponent of h, however, is unknown. What has often been proposed is that the film strength scales inversely with the film thickness [2–5], but experiments are not conclusive. An important reason for variations in scaling is that the response is sensitive to the effectiveness of the interface in blocking slip and to the stiffness of the substrate. At some interfaces, dislocations may be able to pass through the interface relatively easily, at other interfaces dislocations may be able to glide along the interface. Here we focus on interfaces that are elastic and are

*Corresponding author. Email: E.van.der.Giessen@RuG.nl

Philosophical Magazine
ISSN 1478–6435 print/ISSN 1478–6443 online
http://www.tandf.co.uk/journals
DOI: 10.1080/14786430500036611

effective in blocking slip both across and along the interface. Moreover, we confine attention to single crystal films.

Dislocation dynamics simulations of plasticity in single crystal thin films [6, 7] show a size-dependent response for films thinner than roughly one micrometer. Nicola *et al.* [7] attributed the size effect mainly to the presence of a hard, film thickness-independent boundary layer at the film–substrate interface, caused by dislocation pile-ups. However, a Hall–Petch type scaling law with a coefficient common to the three films considered was not found, suggesting that a thickness-independent boundary layer is not the only cause of the size effect. The high stress found in the thinnest film analysed by Nicola *et al.* [7], with $h = 0.25\,\mu\text{m}$, was explained by a different hardening mechanism.

Due to the decreasing dimensions of microelectronic devices, there is growing interest in the mechanical behaviour of thinner films [8]. In this paper, continuing from Nicola *et al.* [7], we carry out discrete dislocation simulations for films with a thickness ranging from $2\,\mu\text{m}$ to $0.125\,\mu\text{m}$. In addition, we study the difference in hardening between thin and very thin films, as found in the simulations, through a simplified analysis of how the dislocation structure is related to the film stress state. The simulations show that there is a material-dependent threshold thickness below which the size effect is solely determined by the capability of Frank–Read sources to operate in a constrained geometry. Only above this threshold thickness, is the size effect due to the thickness-independent boundary layer.

2. Observations from simulations

The evolution of stress in single crystal thin films on a rigid substrate under thermal loading is simulated using discrete dislocation plasticity. The film is modelled in two dimensions with plane strain conditions imposed in the out-of-plane direction (see figure 1). The single crystal is assumed to be perfectly bonded to a semi-infinite substrate. Stress develops due to thermal mismatch between film and the substrate. The stress in the film is partially relaxed by the glide of edge dislocations that nucleate from sources in the film and glide on three sets of slip systems. Possible dislocation nucleation from the interface is not included in the model, nor is dislocation climb which may occur at high temperatures. We also do not consider partial dislocation absorption or transmission at the interface, but for comparison purposes we present results for an interface that allows for complete dislocation transmission. Details of the method, including constitutive rules, and the problem formulation are given in Van der Giessen and Needleman [9] and in Nicola *et al.* [7].

We present results for five films of thickness $h = 2\,\mu\text{m}$, $1\,\mu\text{m}$, $0.5\,\mu\text{m}$, $0.25\,\mu\text{m}$, and $0.125\,\mu\text{m}$. The single crystal contains three slip systems at 60° relative to each other. The discussion mainly focuses on crystals with the set of slip plane orientations $\phi^{(60)} = \{0^\circ, 60^\circ, 120^\circ\}$ but we also consider crystals with the set of slip plane orientations $\phi^{(30)} = \{30^\circ, 90^\circ, 150^\circ\}$. The simulations start from a stress-free and dislocation-free configuration. The film contains a random distribution of 60 sources/μm^2. The nucleation strength τ_{nuc} of each source is randomly taken out of a Gaussian distribution with average $\tau_{\text{nuc}} = 50\,\text{MPa}$ and standard deviation 10 MPa. A dislocation dipole is generated from the source when the resolved shear stress at the source exceeds the nucleation strength during a given time $t_{\text{nuc}} = 10\,\text{ns}$. The elastic properties of the film are assumed to be isotropic with Young's modulus $E = 70\,\text{GPa}$

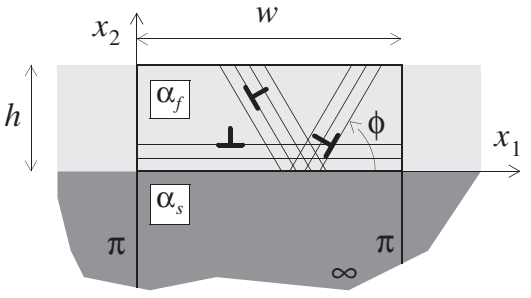

Figure 1. Geometry of the film–substrate problem studied in this paper. A unit cell of width w is analysed and the height of the substrate is taken large enough to represent a half space.

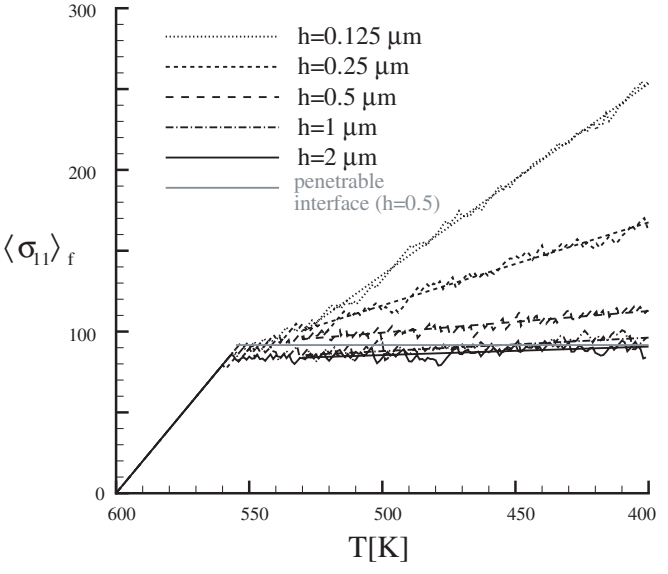

Figure 2. Average stress in the film, $\langle \sigma_{11} \rangle_f$, versus temperature T for films with various thicknesses. Between $T \approx 530\,\mathrm{K}$ and the final temperature, $T = 400\,\mathrm{K}$, the curves have been fitted to straight lines using a standard least-squares algorithm.

and Poisson's ratio $\nu = 0.33$, and are taken to be the same as those of the substrate. During cooling from the stress-free state at 600 K, the stress in the film is driven by the thermal strain $\varepsilon_{\mathrm{th}} = -(1+\nu)\Delta\alpha\Delta T$ arising from the mismatch, $\Delta\alpha = 19 \times 10^{-6}\,\mathrm{K}^{-1}$, between the coefficients of thermal expansion of the film and the substrate.

Figure 2 shows the evolution of the average stress in the film, $\langle \sigma_{11} \rangle_f$, during cooling. For comparison purposes, a curve is also shown for a film for which the interface with the substrate is penetrable for dislocations. After an initial elastic response, the films reach their yield point, which is determined by the weakest source present in the film. With increasing thermal loading, nucleation occurs at other dislocation sources in the film. Plastic relaxation by dislocation motion is quite

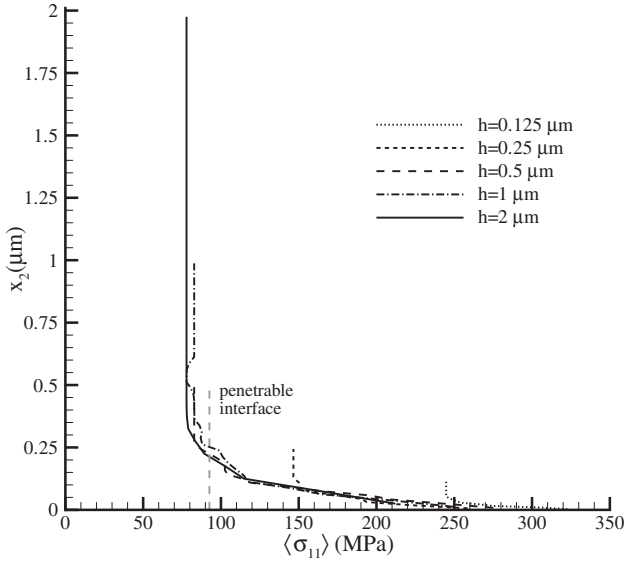

Figure 3. Distribution of the average in-plane stress $\langle\sigma_{11}\rangle$ over the film height in films with an impenetrable interface. The result for a $h = 0.5\,\mu$m film with a penetrable interface is shown for comparison.

effective in all films until a temperature of around 530 K is reached. For the five films with an impenetrable interface, there is a size effect, but it is not as pronounced as during the subsequent cooling. For $T < 530$ K the thinnest two films with an impenetrable interface harden linearly with an increased slope and the size effect becomes more evident. The increased slope arises from the formation of dislocation pile-ups at the film-substrate interface that influence relaxation by inducing a back stress, as discussed by Nicola *et al.* [6, 7] and as also seen in the more recent three-dimensional simulations by Von Blanckenhagen *et al.* [10]. This hardening is essentially kinematic, leading to a strong Bauschinger effect in thermal cycling [11] as observed experimentally by, e.g., Shen and Ramamurty [12].

For a film with $h = 0.5\,\mu$m which has a penetrable interface with the substrate, dislocations can pass through the interface where they are absorbed into the substrate, leaving displacement steps at the interface. In this case, plastic flow continues with the average stress remaining essentially constant at the yield stress. Once nucleated, dislocation pairs glide until one dislocation leaves the film from the free surface and the other enters the penetrable interface. Dislocations do not accumulate in the film as for films with an impenetrable interface, and therefore there is no back stress, no hardening and no size effect.

Figure 3 shows the variation in stress σ_{11} averaged along the x_1 direction over the film height. This average is denoted by $\langle\sigma_{11}\rangle$ and is uniform in the film with a penetrable interface with the substrate. All other films exhibit a boundary layer where $\langle\sigma_{11}\rangle$ increases near the film–substrate interface and an almost homogeneous stress state in the rest of the film.

The line indicating the stress profile in the film with a penetrable interface intersects the curves for the three thicker films. We take this intersection as the separation point between the boundary layer and the zone of homogeneous stress in these films (subsequently referred to as the bulk). For the two thinner films, we define the bulk

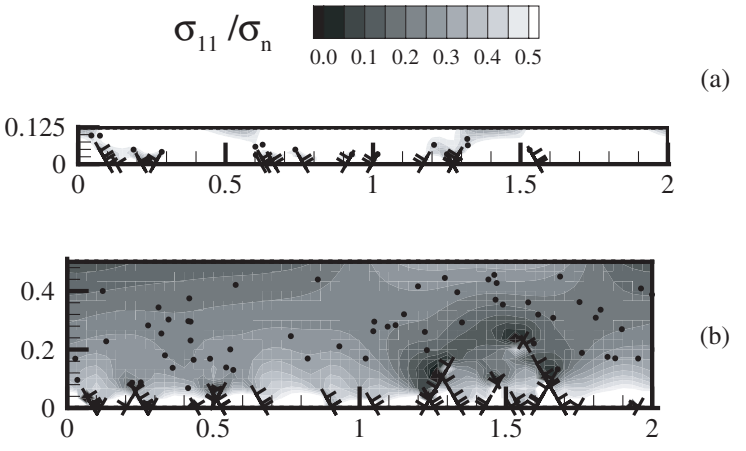

Figure 4. Distribution of dislocations (⊥) and sources (•) in films with thickness (a) $h=0.125\,\mu m$ and (b) $h=0.5\,\mu m$ at final temperature, $T=400\,K$, superimposed on contours of σ_{11}.

as the zone next to the free surface, where $\langle\sigma_{11}\rangle$ is constant (and denoted by $\langle\sigma_{11}\rangle_b$), and the boundary layer as the zone close to the interface were there is a stress gradient. While the three thicker films have approximately the same value of stress in the bulk ($\langle\sigma_{11}\rangle_b \approx 80\,MPa$), the bulk stress level in the two thinner films is much higher ($\langle\sigma_{11}\rangle_b = 145\,MPa$ for the film with $h=0.25\,\mu m$ and $\langle\sigma_{11}\rangle_b = 245\,MPa$ for the film with $h=0.125\,\mu m$). The boundary layer thickness, h_l, is approximately the same in the two thicker films ($h_l=0.25\,\mu m$), but is smaller in the two thinner ones ($h_l \approx 0.1\,\mu m$ for $h=0.25\,\mu m$ and $h_l \approx 0.05\,\mu m$ for $h=0.125\,\mu m$). The thinnest film considered is actually thinner than the boundary layer in the thicker films.

Figure 4 shows the stress state reached at $T=400\,K$ and the corresponding dislocation distribution for the films with $h=0.5$ and $0.125\,\mu m$. Black dots indicate the positions of Frank–Read sources (recall that their density is independent of h). The stress is normalized by the elastic stress

$$\sigma_n = \frac{E}{(1-\nu^2)}\varepsilon_{th} = -\frac{\Delta\alpha E \Delta T}{(1-\nu)}$$

which, for $\Delta T=-200\,K$, is $\sigma_n = 397\,MPa$ for the chosen material parameters. From a given range of contour levels, a comparison can be made between the stress state in the two films, with two differently stressed regions seen in the thicker film. But, of course, a quantitative measure of the size and intensity of the boundary layer cannot be obtained directly from these contour plots.

The analysis of the dislocation structure at $T=400\,K$ gives a better understanding of the stress profiles in figure 3. What is common to the two films in figure 4 is that dislocations have piled up against the film–substrate interface and that only the slip planes at 60° and 120° have been active. The main differences between the dislocation structures in the two films are the dislocation density and the density and length of the dislocation pile-ups. These quantities are listed in table 1, together with the average stress in the films and the stress in the film bulk. The dislocation density for the three thicker films ($h=2\,\mu m$, $1\,\mu m$ and $0.5\,\mu m$) is inversely proportional to the film thickness but for the two thinner films the dislocation density does

Table 1. Features of the results for single crystal films with the slip plane set $\phi^{(60)} = \{0^\circ, 60^\circ, 120^\circ\}$ for various film thicknesses.

h (μm)	0.125	0.25	0.5	1	2
Average stress $\langle\sigma_{11}\rangle_f$ (MPa)	253	167	113	96	90
Bulk stress $\langle\sigma_{11}\rangle_b$ (MPa)	245	147	82	82	78
Dislocation density ρ (μm^{-2})	124	102	64	33	16.5
Pile-up density ρ_p (μm^{-2})	56	40	18	8	4.5
Max pile-up length (μm)	0.045	0.115	0.221	0.250	0.312
Boundary layer thickness h_l (μm)	0.05	0.13	0.250	0.245	0.245
Bulk stress σ_b (MPa) from equation (4)	246	150	87	87	77
Interface stress σ_{int} (MPa) from equation (6)	330	300	310	319	310

not correlate with film thickness. In the thinner films fewer dislocation dipoles have been available to relax the stress, explaining the higher average stress in these films (see also Nicola *et al.* [7]). The reduced nucleation activity in the very thin films is caused by the proximity of the dislocation sources to the film–substrate interface: the length of dislocation pile-ups is limited by the distance between the point source and the interface. The longest pile-up in the film of thickness $h = 1\,\mu m$ is 0.25 μm; obviously such a long pile-up cannot form in a film with $h = 0.125\,\mu m$. In addition, sources that are very close to the interface, and thus to the dislocation pile-ups, are affected by the back stress associated with the pile-ups, which delays the nucleation events [7]. The back stress on a nucleation source close to the interface is mainly caused by the pile-up generated by the source itself. In section 3 we analyse in more detail how the dislocation structure is related to the stress state in the film.

3. Characterization of stress state

3.1. *Stress state in the film bulk*

As shown in figure 3, the average in-plane stress at final temperature, $T = 400\,K$, in the bulk of all films is homogeneous and lower than the elastic stress, $\sigma_n = 397\,MPa$. The stress in the bulk has been relaxed by the glide of dislocation dipoles during the thermal history. One dislocation out of each dipole has left the film through the free surface but the other is still in the film, piled up against the interface. The density of dislocations that have contributed to the relaxation of the film is therefore known from the final dislocation density.

Stress relaxation is mainly given by dislocation glide on the slip planes with $\phi = 60^\circ$ and $\phi = 120^\circ$. Dislocation activity on the slip planes parallel to the interface is very limited, since their Schmid factor is zero. Figure 5a gives a schematic representation of the relaxation process: opposite signed dislocations move on the slip planes, one towards the free surface, the other towards the interface with the substrate. The groups of piled-up dislocations in figure 5a can be approximated by two parallel arrays of dislocations, each having Burgers vector of length $b\cos\phi$ but in one array pointing in the x_1 and in the other array in the $-x_1$ direction.

The stress field of a single array of $b\cos\phi$ with Burgers vector in infinite space (see figure 6) can be calculated analytically (for the complete derivation

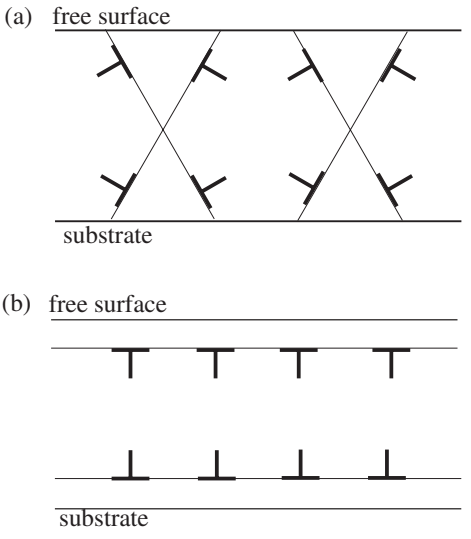

Figure 5. (a) Schematic representation of dislocations gliding on slip planes $\phi = 60^\circ$ and $\phi = 120^\circ$. (b) Dislocation structure equivalent to the one in figure (a), obtained by composing the dislocation Burgers vectors; the Burgers vector of each dislocation in the array is $b\cos\phi$.

see, e.g., Van der Giessen and Needleman [9]):

$$\sigma_{11} = \frac{Eb\cos\phi}{4d(1-\nu^2)}\frac{1}{\cosh 2\pi\eta - \cos 2\pi\xi}\left[2\sinh 2\pi\eta + 2\pi\eta\frac{1-\cos 2\pi\xi\cosh 2\pi\eta}{\cosh 2\pi\eta - \cos 2\pi\xi}\right], \quad (1)$$

where d is the spacing between dislocations, and $\xi = X/d$ and $\eta = Y/d$ are local coordinates of the point were σ_{11} is calculated (see figure 6). This stress, averaged over ξ for any value of $\eta > 0$, is

$$\langle\sigma_{11}\rangle_\xi(\eta) = -\frac{Eb\cos\phi}{2d(1-\nu^2)}. \quad (2)$$

The effect of the array near the free surface is the same, so that the average stress between the two arrays of dislocations in figure 5b is given by

$$\sigma_d = -\frac{Eb\cos\phi}{d(1-\nu^2)}. \quad (3)$$

On average, the effects of the two arrays outside the band cancel. If the dislocation arrays are moving in a film, the stress state in the part of the film where glide has already occurred is $\sigma_n + \sigma_d$ and in the rest of the film it is just the elastic stress σ_n. The relaxation process is complete when one of the arrays reaches the interface and the other the free surface. Then the bulk comprises the entire film and the average stress is $\sigma_b = \sigma_n + \sigma_d$ everywhere in the film, i.e.

$$\sigma_b = \sigma_n - \frac{Eb\cos\phi}{d(1-\nu^2)} = \sigma_n - \frac{\rho hEb\cos\phi}{(1-\nu^2)} \quad (4)$$

where ρ is the density of dislocations inside the film.

The same result can be obtained by considering each dislocation at the interface as an inserted atomic half plane of Burgers vector $b\cos\phi$. The plastic strain caused

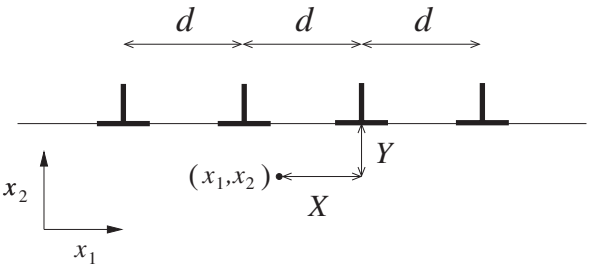

Figure 6. Infinite array of edge dislocations spaced by d.

by inserting an array of such half planes at a spacing d is $\varepsilon_p = b\cos\phi/d$. This strain partly accommodates the applied thermal strain ε_{th}. Accordingly, the bulk stress can be expressed as

$$\sigma_b = \frac{E}{(1-\nu^2)}\left[\varepsilon_{th} - \varepsilon_p\right] = \frac{E}{(1-\nu^2)}\left[(1+\nu)\Delta\alpha\Delta T - \frac{b\cos\phi}{d}\right] \tag{5}$$

which, with $\rho = 1/hd$, is identical to equation (4).

Comparison between the values of σ_b obtained from equation (4), using the values of ρ from the simulations, and $\langle\sigma_{11}\rangle_b$ computed during the simulations shows very good agreement (table 1). We conclude that the density of dislocations in the quantity ρh together with the orientation of the Burgers vectors is sufficient to determine the average stress state in the film bulk. In table 1, the value of ρh is $32\,\mu m^{-1}$ for the thicker films, and only $26\,\mu m^{-1}$ and $16\,\mu m^{-1}$ for the two thinnest films. As mentioned previously, sufficient dislocations are not nucleated in the thinner films to relax the film bulk.

3.2. *Stress state in the boundary layer*

By comparing figure 3 and figure 4 it can be seen that the size of the boundary layer is determined by the length of the dislocation pile-ups (see also table 1). The value of $\langle\sigma_{11}\rangle(x_2)$ is maximum at the interface, where the lead dislocations of the pile-ups are located. At the interface, the effect of these dislocations is dominant. The dislocation array formed by the lead dislocations of all pile-ups produces a stress state that can again be described by equation (3). The stress at the interface is calculated as

$$\sigma_{int} = \sigma_n - \frac{\rho_p hEb\cos\phi}{(1-\nu^2)} \tag{6}$$

where the pile-up density ρ_p is the number of dislocations that are located exactly at the interface divided by the cell area hw.

The values, calculated using equation (6) (listed in table 1), are somewhat larger than the values in figure 3 because the stress in that figure is not calculated exactly at the interface, but through integration points close to the interface. The stress rapidly decreases with distance from the interface until it reaches the bulk stress. The stress gradient is not constant in the boundary layer, but decreases as the bulk is approached, where only the last dislocations of a few long pile-ups contribute to it. Dislocation pile-ups are shorter in the films thinner than the threshold thickness, so that the boundary layer thickness in these films is reduced. However, even though the

boundary layer thickness is reduced for these thinner films, the average stress, both in the boundary layer and in the bulk, is higher than in the films thicker than the threshold film thickness. For films thinner than the threshold film thickness, the strengthening mechanism is not a boundary layer effect.

3.3. *Validity of the Hall–Petch relation*

First focus attention on the thicker films, $h \geq 0.5\,\mu\text{m}$, and assume a relation of the form

$$\sigma = \sigma_0 + kh^{-n}, \tag{7}$$

where σ is the film average stress. Then, take $\sigma_0 = \sigma_b \approx 80\,\text{MPa}$, since the thicker films have a similar stress state in the bulk. The exponent n is readily determined by considering the ratio of the values $\sigma - \sigma_0$ for $h = 1\,\mu\text{m}$ and $0.5\,\mu\text{m}$ using the values of $\langle\sigma\rangle_f$ from table 1 for σ in equation (7). This yields $n = 1$, and subsequently we obtain $k = 16\,\text{MPa}\,\mu\text{m}$. As a check, using these parameter values, equation (7) predicts $\sigma = 88\,\text{MPa}$ for the film with $h = 2\,\mu\text{m}$, which is very close to the value of $\langle\sigma\rangle_f = 90\,\text{MPa}$ obtained from the simulation (see table 1).

Alternatively, the average stress in the film can be seen as the weighted sum of the stress in the film bulk and the average stress in the boundary layer, i.e.

$$\sigma = \sigma_b \frac{1 - h_l}{h} + \sigma_l \frac{h_l}{h}, \tag{8}$$

where σ_l and h_l indicate the boundary layer average stress and the boundary layer thickness, respectively. Equation (8) can be rewritten in the form of equation (7) as

$$\sigma = \sigma_b + (\sigma_l - \sigma_b)h_l/h, \tag{9}$$

so that $k(\sigma_l - \sigma_b)hl$ and $n = 1$.

Equation (9), which is essentially a rule-of-mixtures relation, holds for films of any thickness. It can be regarded as the Hall–Petch type relation, equation (7), with $n = 1$ when the coefficients are independent of the film thickness, which, in our analyses, only holds if the film thickness exceeds a material-dependent thickness. For the three thicker films analyzed here, k and $\sigma_0 \approx \sigma_b$ in equation (7) are constant and can be considered material parameters. On the other hand, for thinner films, k and $\sigma_0 \approx \sigma_b$ depend on the film thickness: the stress levels in the bulk and in the boundary layer increase with decreasing film thickness, while the thickness of the boundary layer decreases. Thus, for these thinner films a Hall–Petch type relation no longer holds.

The values of the film thickness, above which the films will behave according to equation (7) with a constant k and σ_b, depend on all parameters which affect the dislocation density in the films, such as the density and strength of the nucleation sources.

4. Crystal orientation

The response of a single crystal depends on its orientation. Figure 7 shows the stress profiles for simulations of four films having thicknesses ranging from $0.125\,\mu\text{m}$ to $1\,\mu\text{m}$ and slip plane orientations $\phi^{(30)} = \{30^\circ, 90^\circ, 150^\circ\}$. Table 2 summarizes features of the results.

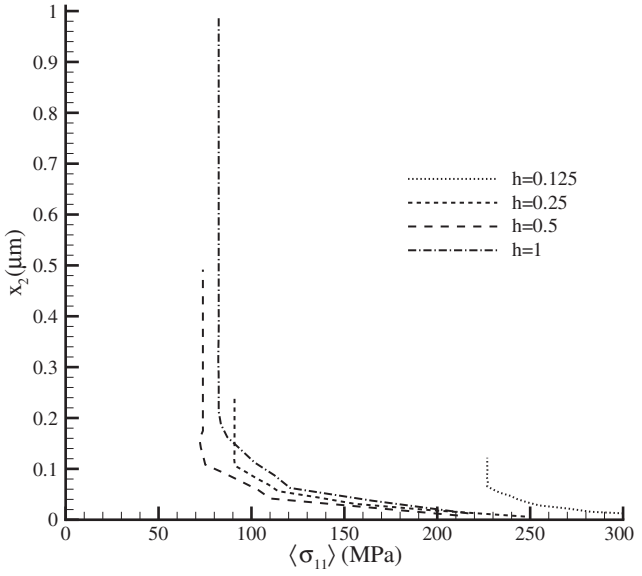

Figure 7. Distribution of the average in-plane stress $\langle\sigma_{11}\rangle$ over the film height in films having various thicknesses with the slip plane orientation set $\phi^{(30)} = \{30^\circ, 90^\circ, 150^\circ\}$.

Comparison of tables 1 and 2 reveals that the average and bulk stress in the single crystals with the slip planes set $\phi^{(30)}$ is lower than in the crystals with the slip plane set $\phi^{(60)}$. Nevertheless, the dislocation densities for the $\phi^{(30)}$ films are lower than those in the $\phi^{(60)}$ films. Thus, with slip planes oriented at $\{30^\circ, 90^\circ, 150^\circ\}$ a dislocation density lower than that in a crystal with slip planes oriented at $\{0^\circ, 60^\circ, 120^\circ\}$ is needed to give the same relaxation. For films thicker than the threshold thickness, this can be rationalized through equation (4): $\cos\phi$ is larger for $\phi = 30^\circ$ than for $\phi = 60^\circ$. Due to the different inclination of the slip planes, the same length of dislocation pile-ups gives a thinner boundary layer for the slip plane orientation set $\phi^{(30)}$ than for the slip plane orientation set $\phi^{(60)}$.

Particularly interesting is the behaviour of the film with thickness 0.25 μm. In section 3.3, it was seen that for this film thickness a Hall–Petch type relation equation (7) was not followed with the slip plane set $\phi^{(60)}$ because of insufficient dislocation nucleation. With the slip plane set $\phi^{(30)}$, however, fewer dislocations are required for stress relaxation in the film. Hence, for $\phi^{(30)}$ the film with $h = 0.25\,\mu\text{m}$ does not deviate from the behaviour described by equation (7). However, in the bulk of the thicker films with slip plane set $\phi^{(30)}$ the stress magnitude is approximately the same as in the crystal with $\phi^{(60)}$ ($\sigma_b \approx 80$ MPa), even though there is more scatter in the results. The constants k and n in equation (7) can be regarded as depending on orientation, and therefore have a different value with slip planes oriented at $\{30^\circ, 90^\circ, 150^\circ\}$. Retaining the $\phi^{(60)}$ value $n = 1$, we obtain a least-squares fit to the $\phi^{(30)}$ data for $k = 10.6\,\text{MPa}\mu\text{m}$ and $\sigma_0 = 72$ MPa. With these values, equation (7) gives $\sigma = 84$ MPa, 93 MPa and 114 MPa for the films with $h = 1\,\mu\text{m}$, 0.5 μm and 0.25 μm, respectively. However, $n = 0.5$ and $k = 10\,\text{MPa}\mu\text{m}^{0.5}$ in (7) yield $\sigma = 90$ MPa, 94 MPa and 100 MPa for the same thickness when $\sigma_0 = 80$ MPa. In either case the agreement with the film averages $\langle\sigma_{11}\rangle_f$ of table 2 is not as good in section 3.3 for the orientation $\phi^{(60)}$.

Table 2. Features of the results for single crystal films with slip plane orientations $\phi^{(30)} = \{30°, 90°, 150°\}$ for various film thicknesses.

h (μm)	0.125	0.25	0.5	1
Average stress $\langle\sigma_{11}\rangle_f$ (MPa)	248	114	85	91
Bulk stress $\langle\sigma_{11}\rangle_b$ (MPa)	227	91	74	82
Dislocation density ρ (μm^{-2})	80	72	40	19
Pile-up density ρ_p (μm^{-2})	24	22	12	4.5
Maximum pile-up length (μm)	0.046	0.094	0.159	0.169

5. Concluding remarks

Stress relaxation of single-crystal thin films of various thicknesses on a semi-infinite substrate has been simulated using discrete dislocation plasticity. The simulations show that:

- if the film-substrate interface is taken to be perfectly penetrable for dislocations, the stress that the substrate imposes on the film relaxes to a level that depends only on the strength of the weakest nucleation source, independently of the film thickness;
- if the film-substrate interface is impenetrable, stress relaxation is not as efficient as in films with a penetrable interface, because dislocations cannot glide through the interface, but pile-up against it, forming a boundary layer characterized by a high stress gradient. The boundary layer is a transition zone between the high stress state at the film-substrate interface and the more relaxed stress state near the free surface.
- There is a threshold thickness above which films have a boundary layer with thickness-independent size and average stress. The stress in the rest of the film is very low. Dislocation activity is as intense as in films with a perfectly penetrable interface with the substrate, so that the stress relaxation in the film bulk is quite good and independent of the film thickness. The size effect in these films is caused by the fact that the size of the boundary layer does not scale with the film thickness.
- In films thinner than a threshold thickness, which depends on the material and on the crystal orientation, nucleation is hindered by a geometrical constraint, i.e. the proximity of sources to the interface. The thinner the film, the lower the dislocation activity. Both the average stress in the boundary layer and the stress in the film bulk increase with decreasing dislocation density. The boundary layer thickness depends on the length of the pile-ups and decreases with film thickness. So, with decreasing film thickness the boundary layer becomes thinner but the stresses both in the boundary layer and in the bulk of the film increase. The size effect in these very thin films is nucleation-controlled and is more pronounced than in the thicker films.

Acknowledgements

This research was carried out under project number MS97007 in the framework of the Strategic Research Program of the Netherlands Institute for Metals Research in the Netherlands (www.nimr.nl). A.N. is pleased to acknowledge support from the

Materials Research Science and Engineering Center on *On Micro-and-Nano-Mechanics of Electronic and Structural Materials* at Brown University (NSF Grant DMR-0079964).

References

[1] E. Arzt, Acta mater. **46** 5611 (1998).
[2] L.B. Freund, J. appl. Mech. **43** 553 (1987).
[3] R. Venkatraman and J.C. Bravman, J. Mater. Res. **7** 2040 (1992).
[4] W.D. Nix, Scripta mater. **39** 545 (1998).
[5] G. Dehm, T. Wagner, T.J. Balk, E. Arzt and B.J. Inkson, J. Mater. Sci. Technol. **18** 113 (2002).
[6] L. Nicola, E. Van der Giessen and A. Needleman, Mater. Sci. Engng A **309–310** 274 (2001).
[7] L. Nicola, E. Van der Giessen and A. Needleman, J. appl. Phys. **93** 5920 (2003).
[8] L.B. Freund and S. Suresh, *Thin Film Materials: Stress, Defect Formation and Surface Evolution* (Cambridge University Press, Cambridge, 2003).
[9] E. Van der Giessen and A. Needleman, Model. Simul. Mater. Sci. Engng **3** 689 (1995).
[10] B. Von Blanckenhagen, P. Gumbsch and E. Arzt, Acta mater. **52** 773 (2004).
[11] L. Nicola, E. Van der Giessen and A. Needleman, in *Solid Mechanics and Its Applications*, Vol. 114, edited by S. Ahzi, M. Cherkaoui, M.A. Khaleel, H.M. Zbib, M.A. Zikry, and B. LaMatina (Kluwer Academic Publishers, Dordrecht, 2004).
[12] Y. Shen and U. Ramamurty, J. appl. Phys. **93** 1806 (2003).